Determination of the lateral Xe-Xe potential in a single xenon layer adsorbed on Cu(110) from surface phonon dispersion measurements

Ch. Boas,[1] M. Kunat,[1] U. Burghaus,[1] B. Gumhalter,[2] and Ch. Wöll[1]
[1]*Lehrstuhl für Physikalische Chemie I, Ruhr-Universität Bochum, D-44780 Bochum, Germany*
[2]*Institute of Physics of the University, P.O. Box 304, 10001 Zagreb, Croatia*
(Received 22 January 2003; published 12 August 2003)

The dynamics of high-order $c(26\times2)$ Xe monolayer adsorbed on Cu(110) was determined using high-resolution inelastic He-atom scattering. In addition to the vertically polarized S_1 mode we observed a longitudinally polarized L mode with a small excitation probability, which has been seen before for Xe adlayers on the two other low-index Cu single-crystal surfaces Cu(100) and Cu(111). The L mode exhibits a zone-center gap of 0.55 ± 0.15 meV along the [001] direction, which allows us to estimate the corrugation of the Xe-Cu(110) potential-energy surface. The dispersion of the L mode reveals an anomaly in the interaction between adsorbed Xe atoms. Likewise, in previous studies of Xe monolayers on Cu surfaces, the data analysis reveals an anomalous softening of the Xe-Xe interaction.

DOI: 10.1103/PhysRevB.68.075403 PACS number(s): 68.35.Ja, 63.22.+m, 34.50.Dy

I. INTRODUCTION

Single layers of noble gases physisorbed on single-crystal surfaces are considered to be ideal model systems with regard to a detailed understanding of the structure and dynamics of adsorbates.[1] The general interest in these systems is based on the assumption that the interaction between noble-gas atoms is only slightly modified when deposited on a metal surface. However, recent experimental results on the anomalously small force constants describing the coupling of Xe atoms adsorbed on different Cu surfaces have challenged this assumption.[2,3] A lattice-dynamical analysis of a longitudinal mode in Xe monolayers adsorbed on Cu(100) and on Cu(111) reveals numerical values for the force constants coupling the adjacent atoms that are only 30% of the values expected from the corresponding precise gas-phase potentials. Recently, however, the interpretation of the experimental data has been challenged by Bruch who suggested a different assignment of the low-energy vibrations seen in the He-atom scattering (HAS) data.[4] In addition, new data on the vibrational properties of noble-gas adlayers adsorbed on Pt(111) were interpreted in terms of a rather good agreement with theoretical expectations.[5] With regard to the anomaly in the Xe-Xe potential for monolayers on Cu substrates it has also remained unclear why the anomaly was not observed for Cu(110) in the previous work by Zeppenfeld *et al.*[6,7] Here we report the results of a reinvestigation of the $c(26\times2)$ overlayer of Xe on Cu(110). Our new data strongly suggest that the earlier data reported in Refs. 6 and 7 have to be reassigned. Our precise determination of the L mode for this surface reveals the same anomalies seen for the two other low-index Cu surfaces. In addition, the fact that the present surface exhibits a twofold symmetry only allows for a clear distinction between the shear-horizontal and longitudinal modes, thus fully corroborating our earlier assignment for the case of Cu(111) and Cu(001) surfaces. Furthermore, from the zone-center phonon gap observed in the present work along the [001] direction, we can estimate the corrugation of the Xe-Cu(110) potential-energy surface along this direction.

II. EXPERIMENTAL SETUP

The experiments to be presented here were performed in a high-resolution helium-atom surface scattering apparatus (GURKE). The experimental setup has been described in detail elsewhere,[8] so only a brief description of the main characteristics will be given here. The energy of the nearly monoenergetic supersonic helium-atom beam with a typical full width at half maximum (FWHM) of $\Delta E/E\cong2\%$ is determined by the nozzle temperature, which can be varied in the range of $T_N=40-500$ K ($E_i\cong10-120$ meV). The scattered helium atoms are detected at a fixed total scattering angle of $\Theta_{SD}=90.5°$ between incoming and outgoing beams with a homemade magnetic mass spectrometer, mounted at a distance of 1.08 m from the target. Angular diffraction scans are measured by rotating the crystal around an axis perpendicular to the scattering plane in the steps of $\Delta\Theta_i=0.05°$ (polar angle). Energy-loss spectra are recorded using a time-of-flight (TOF) technique. The overall angular resolution amounts to about $\Delta\Theta\cong0.25°$ and the resolution in the energy-loss measurements to $\delta(\Delta E)\leqslant0.3$ meV (see Smilgies and Toennies[9] and Hinch *et al.*[10]). Both values depend on the various machine parameters: the values given above are valid for the energy range of $E_i=10-25$ meV. The TOF setup was calibrated by using a molecular beam of HD seeded in He (10% H_2, 10% D_2, 80% He passed through a heated Mg reactor) and determining the well-known excitation energy of the first (11.06 meV) and second (33.12 meV) rotational states of the HD molecule.[11] For the present experiments it was essential to be able to rapidly cool down the crystal (400–40 K in 10 min) in order to avoid a contamination of the sample. During the experiments reported here, the base pressure in the scattering chamber was in the low-10^{-11}-mbar-pressure range. The cooling to 30 K was accomplished by using a liquid-helium cold finger. The temperature measurement accuracy $\Delta T_S=\pm5$ K of the absolute surface temperature, measured with a Ni-NiCr (K-type) thermocouple attached to the side of the specimen, was determined *in situ* with a calibrated Si diode (Lakeshore DT-

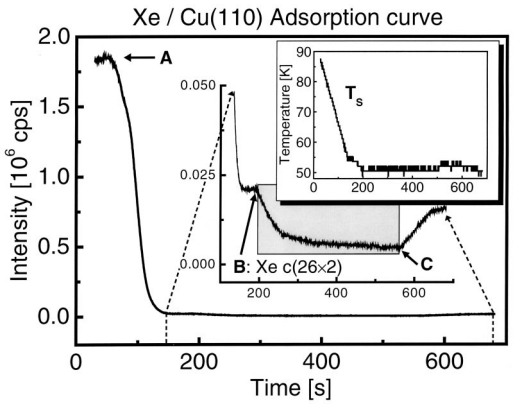

FIG. 1. Intensity of the specularly reflected He beam recorded during Xe exposure (Xe pressure: 1×10^{-8} mbar) and slowly decreasing sample temperature ($T_S=94-50$ K; He beam energy $E_i=10.7$ meV). (A) Beginning of the adsorption process at $T_S=81$ K. (B) Formation of the Xe $c(26\times2)$ phase in a narrow temperature interval from $T_S=55-52$ K. The reflectivity of the Xe adlayer is reduced to 1% of the reflectivity of the clean surface. (C) End of Xe exposure and reformation of the (26×2) overlayer. Gray rectangle: bilayer formation below $T_S=52$ K at a Xe pressure of 1×10^{-8} mbar (Refs. 33 and 34). The inset shows the variation of the sample temperature with time.

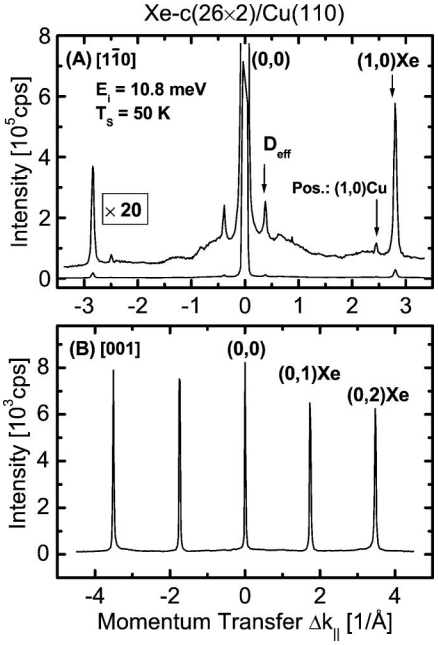

FIG. 2. He-atom diffraction scans of the well-defined, highly ordered commensurate Xe $c(26\times2)$ structure recorded along the two high-symmetry directions $[1\bar{1}0]$ (A) and [001] (B) of the copper fcc (110) surface at an incident He energy of 10.8 meV and a sample temperature of 50 K. Small peaks at the $(\pm1,0)$ Cu position imply that the Xe overlayer has only a small corrugation amplitude equal to the substrate corrugation in $[1\bar{1}0]$ direction. In the [001] direction Xe diffraction peaks fit perfectly to the underlying substrate structure.

471-SD) and by recording thermal desorption spectra of multilayers of *n*-alkanes.[12,13]

The mechanically polished Cu(110) crystal was first aligned to within 0.1°, then cleaned *in situ* in vacuum with multiple cycles of argon-ion sputtering (1 μA cm^{-1}, 700 eV), and finally annealed at $T_S=900$ K. After this preparation no contamination could be detected with x-ray photoemission spectroscopy (less than 5% of a monolayer for carbon containing species) and the helium diffraction pattern showed intense diffraction peaks and a low diffuse background. Exposure to Xe was carried out by using an effusive source mounted at a distance of 7 mm in front of the crystal surface. During exposure, the pressure inside the chamber increased to 1×10^{-8} mbar: the pressure at the surface is estimated to be about 2 orders of magnitude above this value.

III. RESULTS

A. Structure

As discussed by Zeppenfeld *et al.*[14] in their detailed analysis of the various temperature- and coverage-dependent high commensurate (HOC) Xe overlayers on Cu(110), the $c(26\times2)$ phase is the most stable structure in the temperature range from $T_S=60$ to 40 K. Below 40 K the bilayer formation starts and special care has to be taken to avoid bilayer formation at lower temperatures. The adsorption of Xe on the Cu(110) surface was monitored by recording the intensity of the specular He $I_{(0,0)}$ beam versus time (i.e., the surface reflectivity). In Fig. 1 we display a typical $I_{(0,0)}$ vs time plot, recorded using a Xe background pressure of 1×10^{-8} mbar and a cooling rate of $\delta T_S/\delta t=0.3-0.1$ K/s (the substrate temperature as a function of time is shown in the inset of Fig. 1). The results reveal the onset of Xe adsorption at $T_S=81$ K (*A*) and the formation of a terrace in the adsorption curve in the narrow temperature interval from $T_S=55\geqslant T_S\geqslant52$ K (*B*). The latter feature could be related to the formation of a Xe $c(26\times2)$ phase as evidenced by the He diffraction scans. For the following experiments the Xe adlayer was prepared by adsorption at a fixed temperature of 53 K, yielding a well-ordered $c(26\times2)$ HOC structure. When monolayer coverage was reached, the Xe gas was pumped off and the crystal was cooled to 30–35 K before the inelastic He scattering data were recorded. To maintain the quality of the adlayer over longer periods of time (typically 6–8 h) the surface was periodically annealed to 55 K to remove bilayer Xe formed by adsorption from the residual gas. In Fig. 2 typical angular distributions measured along the two high-symmetry directions of the Cu(110) surface are displayed. Along the [001] direction (*B*) the relative intensities $I_{(0,1)}\cong I_{(0,2)}$ of the $(\pm0,1)$ Cu and $(\pm0,2)$ Cu diffraction peaks with respect to the specularly reflected intensity $I_{(0,0)}$, $I_{(0,1)}/I_{(0,0)}\cong1$ were found to be significantly larger than for the clean surface where $I_{(0,1)}/I_{(0,0)}\leqslant1/35$. No new diffraction peaks are seen along this azimuth. Along the $[1\bar{1}0]$ direction (*A*) a more complicated scenario is observed. In addition to the small diffraction peaks located at the (1,0) and $(-1,0)$ positions of the clean Cu(110) substrate at $\Delta k_{\|}=\pm2.46$ Å^{-1}, intense diffraction peaks labeled $D_{\rm eff}$ are detected at $\Delta k_{\|}=\pm0.38$ Å^{-1} and a new peak labeled (1,0) Xe is seen at $\Delta k_{\|}=\pm2.84$ Å^{-1}. The positions and intensities of

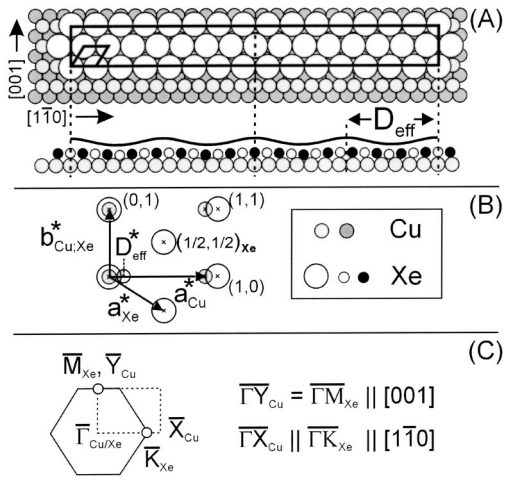

FIG. 3. (A) Schematic model of the HOC $c(26\times2)$ Xe overlayer on Cu(110). In the top view the first and second substrate layers (gray and dark gray) are shown together with the Xe adlayer. The HOC Xe adlayer unit cell and the primitive cell of the quasihexagonal lattice (solid rectangle and parallelogram) are also shown. The lower sketch of the side view (first and second rows of the HOC structure are marked as small white and black balls) illustrates the small modulation of the corrugation profile introduced by the Xe overlayer. The periodicity D_{eff} of this pattern causes sharp diffraction peaks in the He-atom angular distributions. (B) Image of the reciprocal unit cell of the copper substrate and the quasihexagonal Xe adlayer (see also the He diffraction pattern in Fig. 2). (C) Related Brillouin-zone scheme and high-symmetry directions of the Xe adlayer and Cu(110) substrate structure.

these peaks are directly related to the HOC adlayer structure as explained in the sketch of the real and *k*-phase scheme plotted in Fig. 3. Whereas in the [001] direction the adlayer is in perfect registry with every second row of the Cu substrate, along the [1$\bar{1}$0] direction the Xe atoms form a high-order commensurate structure with the unit cell size amounting to 26 times the Cu-Cu distance [see the solid rectangle in the top view of the sketch shown in Fig. 3(A)]. The resulting quasihexagonal Xe structure [solid parallelogram in Fig. 3(A)] is slightly compressed with respect to an ideal floating two-dimensional (2D) Xe overlayer. Perpendicular to the Cu troughs the Xe-Xe distance is reduced from $a_{\mathrm{Xe}}=4.36-4.40$ Å for the ideal layer to $b_{\mathrm{Xe}}=4.23$ Å (Ref. 3). Parallel to the copper rows the equilibrium Xe-Xe distance is slightly relaxed to $a_{\mathrm{Xe}}=4.42$ Å, corresponding to a position of the (1,0) Xe peak in the He diffraction scan at 2.84 Å^{-1} [compare Fig. 3(B)]. The small long-range corrugation resulting from the misfit between the Xe HOC layer and the substrate is shown in the side view (solid line) of Fig. 3(A). The large periodicity of this modulation, $D_{\mathrm{eff}}=16.58$ Å, gives rise to the diffraction peak labeled D_{eff} in the He diffraction pattern. For the schematic model depicted in Fig. 3(A) we assume an on-top adsorption site of the Xe atoms in accordance with recent experimental results from low-energy electron diffraction studies of Xe on Cu(111) and Kr on Cu(110) (Refs. 15 and 16).

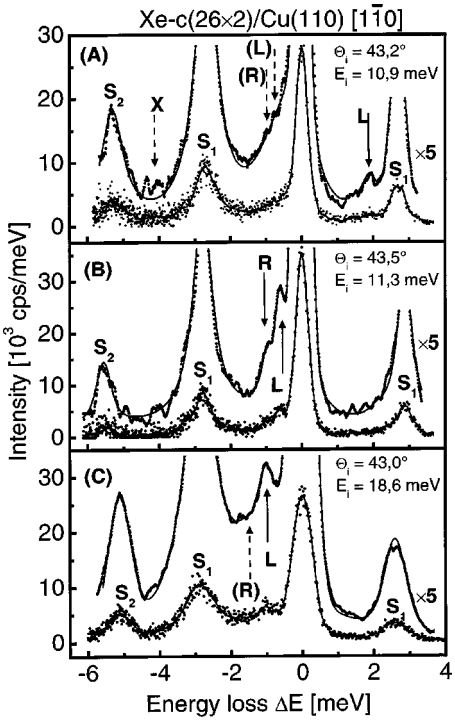

FIG. 4. Series of He-atom energy-loss spectra recorded for the $c(26\times2)$ Xe overlayer on Cu(110) along the $\overline{\Gamma X}$ direction at a sample temperature of 35 K. The lower curves show the raw (dots) and smoothed (solid line) data, respectively. The experimental data (single points) were smoothed using the Savitzky-Golay algorithm, assuming a theoretical resolution corresponding to 90% of the elastic peak FWHM (at $\Delta E=0$). The curves shown in the upper parts compare the smoothed spectra (here: dots) with curves (solid lines) obtained from a fit with Gaussian profiles (nonlinear Levenberg-Marquardt routine with Lorentzian minimization).

B. Phonon dispersion: Xe on Cu(110)[1$\bar{1}$0]

Figure 4 shows a series of typical TOF spectra recorded for the $c(26\times2)$ Xe overlayer along the [1$\bar{1}$0] direction ($\overline{\Gamma X}_{\mathrm{Cu}}\|\overline{\Gamma K}_{\mathrm{Xe}}$) for different incident energies E_i and angles of incidence Θ_i. The TOF spectra have been converted from a flight time scale to an energy-transfer scale. Besides the diffuse elastically scattered signal ($\Delta E=0$), the spectrum is dominated by intense peaks located at ±2.63 and -5.25 meV on the energy-gain and -loss sides, respectively. These peaks are assigned to the excitation of collective Einstein-like vibrations of the Xe atoms polarized normal to the surface S_1 and the corresponding first overtone S_2 (Ref. 17). In addition to these strong peaks, a weak but distinct feature labeled *L* can be identified. This feature is located at smaller frequencies than the transverse mode S_1 and reveals a strong variation of the energy with angle of incidence. In analogy to the findings reported for the dynamics of Xe monolayers on the copper (001) and (111) surfaces, we assign this mode to the longitudinally polarized adlayer vibration.[2,3] The weak feature marked *R* is assigned to the substrate Rayleigh wave phonon. The weak feature about $\Delta E=4.3$ meV (labeled *X*) present in some spectra [Figs. 4(A) and 4(C)] is reminiscent of the feature that was also observed in HAS from the

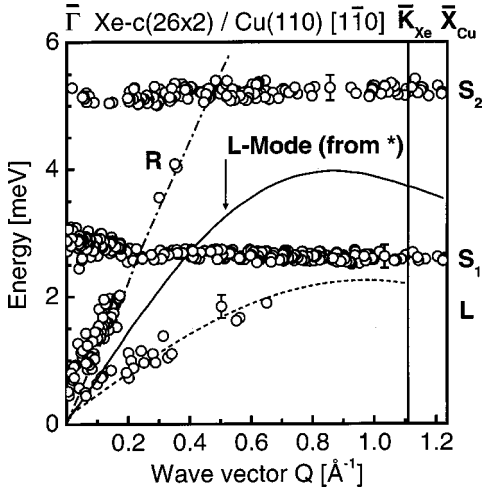

FIG. 5. Phonon dispersion plot of the Xe monolayer in a reduced-zone scheme for the $\overline{\Gamma X}$ direction. The dash-dotted line marks the Rayleigh wave (Ref. 6), whereas the solid line is the calculated *L*-mode dispersion curve taken from Ref. 23. The dotted line corresponds to the dispersive curve of a Xe adlayer with the radial force constant relaxed to 30% of the Xe bulk value and is assumed to be of sinusoidal shape.

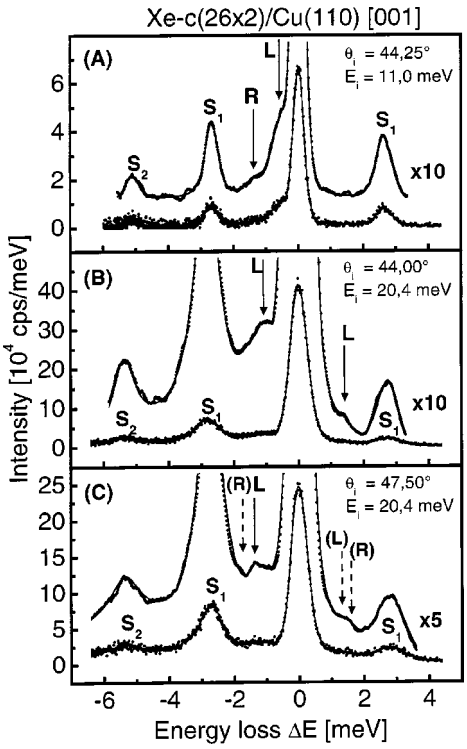

FIG. 6. Series of He-atom energy-loss spectra recorded for the $c(26\times2)$ Xe overlayer on Cu(110) along the $\overline{\Gamma Y}$ direction at a sample temperature of 35 K using different kinematical conditions. Similar to Fig. 4 the lower curves show the raw (dots) and smoothed (solid) data. The upper curves show solid lines obtained using a fitting procedure assuming Gaussian line shapes on top of points corresponding to the smoothed raw data.

Xe(111) surface[18] and assigned to a two-phonon event involving two Rayleigh phonons with wave vectors corresponding to opposite edges of the first Brillouin zone.[2,19,20] In the present He-Xe/Cu(110) scattering system the *L* mode may play the role which the low-energy Rayleigh wave plays in HAS from the Xe(111) surface. However, in view of very low *L*-mode excitation probabilities already for the wave vectors in the first half of the surface Brillouin zone [which is not the case in the He-Xe(111) system], this assignment seems less likely than the one involving localized modes associated with defects present on the Xe surface (cf. discussion in Sec. VI of Ref. 2). For the *L* and *S* modes a precise determination of the peak positions has been carried out by a fitting procedure using Gaussian line profiles (nonlinear Levenberg-Marquardt routine with Lorentzian minimization). The results of the fitting procedure are shown as solid lines in the upper part of the spectra shown in Figs. 4(A)–4(C). Only peaks with intensities clearly above the noise level were considered, and a Gaussian-shaped background was added for higher He atom incident energies.[9,21] The faint features enclosed in parentheses are located at the position expected for Rayleigh- and *L*-mode phonons, but were not—because of their small intensities—included in the fitting procedure. Most of the *L*-mode events are detected at He-atom incident energies below 18.6 meV in the single-phonon excitation regime where the multiphonon background, complicating the identification of the single-phonon peaks, is significantly reduced in intensity. A transition to the multiphonon regime can be seen as a rising background in the spectrum at the bottom of Fig. 4 (Refs. 20 and 22). Figure 5 shows a compilation of phonon peak positions extracted from a large number of TOF measurements (~500), recorded at various He-atom incident energies and incident angles. In order to aid the analysis, all points are plotted in a reduced zone diagram (Fig. 5), where energy and momentum transfer are folded back into the first Brillouin zone. The Cu substrate Rayleigh wave (dash-dotted line) can be easily identified as well as the nearly dispersionless Einstein-like S_1 mode with its second harmonic S_2 located at 2.63 and 5.25 meV, respectively. The avoided crossing of the S_1 and Rayleigh modes at about $Q=0.2$ Å^{-1} could not be resolved. In contrast to previous results,[7] a new highly dispersive phonon branch labeled *L* is seen (dotted line). The intensity of this mode is found to strongly decrease with transferred wave vector so that data points could only be obtained for the first half of the copper surface Brillouin zone. As emphasized by the dotted line, along this direction the *L* mode shows no or only a very small zone center gap: i.e., the curve tends to the origin of the dispersion plot ($E=0$ meV, $Q=0$ Å^{-1}). From the data we obtain an upper limit for a possible phonon gap of 0.2 meV.

C. Phonon dispersion: Xe on Cu(110)[001]

In Fig. 6 a typical series of spectra recorded for the Xe HOC monolayer along the other high-symmetry azimuth of the Cu surface, the [001] direction ($\overline{\Gamma Y}_{Cu}=\overline{\Gamma M}_{Xe}$), is shown. Similar to the spectra along the [1$\bar{1}$0] azimuth, a weak but distinct peak labeled *L* can be identified besides the dominant peaks of the transverse mode S_1 at ±2.63 meV (and its second harmonic S_2 at -5.25 meV). The *L* mode

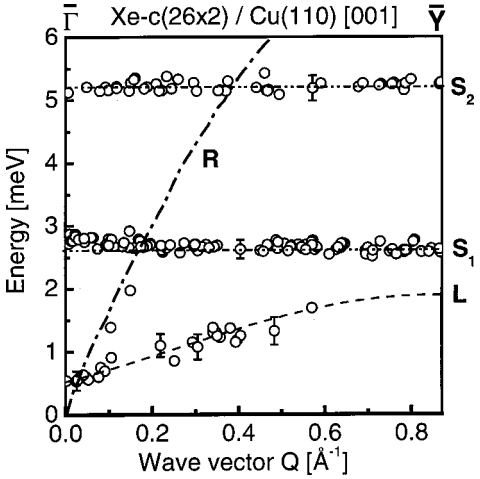

FIG. 7. Phonon dispersion plot of the Xe monolayer in a reduced-zone scheme for the $\bar{\Gamma}\bar{Y}$ direction. The dash-dotted line corresponds to the Rayleigh-wave surface phonon (Ref. 6) of the clean copper substrate. The dashed line is intended to serve as a guide to the eye and indicates the dispersion of the *L* mode.

appears at smaller energies than the more intense S_1 mode, and the precise energy varies strongly with the angle of incidence: i.e., the *L* mode exhibits significant dispersion. In analogy to the situation for Xe on Cu(111) (Ref. 2) and Xe on Cu(100) (Ref. 3) we assign this mode to the longitudinally polarized Xe vibration. Most of the observed weak features (labeled *R* enclosed in parentheses) which energetically coincide with the substrate Rayleigh phonon dispersion curve are too weak to be explicitly included in the peak analysis.

In Fig. 7 the results extracted from a total of 350 TOF spectra are plotted in a reduced-zone scheme. A detailed investigation reveals a rather similar situation to that for the $[1\bar{1}0]$ high-symmetry azimuth discussed above, except that only few peaks which could be assigned to the substrate Rayleigh wave were detected. The most significant difference is the fact that for $Q=0$ the *L* mode extrapolates to a nonzero value, $\omega_L(0)=0.55\pm0.15$ meV. A zone-center phonon gap of similar size, 0.4 meV, was observed previously for a commensurate $(\sqrt{3}\times\sqrt{3})R30°$ monolayers of Xe on Cu(111) (Ref. 2). Here it is also related to the fact that along this direction the Xe overlayer is commensurate with a rather small unit cell (see below).

D. Adsorption of CO on the Xe/Cu surface

In the present work we observe that the He-atom energy-loss peaks assigned to the *L* mode exhibit an intensity which is significantly smaller than that of the *S* mode, in agreement with previous work related to Xe monolayers adsorbed on other two low-indexed Cu surfaces.[2,3] Such a small excitation probability is also in accordance with theoretical results for the excitation probability of differently polarized adsorbate vibrational modes[19,22] and can be related to the fact that this mode exhibits a longitudinal polarization which couples to the He atoms much weaker than the transversely (normal to the surface) polarized *S* mode.[19,22] The present results are,

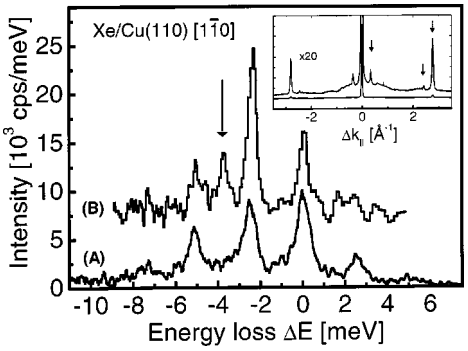

FIG. 8. (A) He-atom energy-loss spectrum recorded for the $c(26\times2)$ Xe overlayer on Cu(110) at a sample temperature of 35 K for an angle of incidence of 36° and at He-atom incident energy of $E_i=18.2$ meV. The inset shows a He-atom angular distribution recorded before the TOF measurements. (B) He-atom energy-loss spectrum taken from Zeppenfeld *et al.* (Ref. 7). The peak at ~3.7 meV (arrow) is absent in the new data.

however, inconsistent with the previous reports on the observation of the *L* mode in this Xe monolayer, where rather intense peaks (excitation probability comparable to the S_2 mode) were reported.[7]

In order to resolve the discrepancy between our measurements and the results reported by Ramseyer *et al.*[23] and Zeppenfeld *et al.*,[7,14] we made several attempts to reproduce the pronounced peak at 3.75 meV seen in their TOF spectra by recording the data under identical kinematical conditions (i.e., $\Theta_i=36.0°$, $E_i=18.8$ meV). Prior to recording He-atom energy-loss spectra, an angular distribution was recorded, which is shown in the inset of Fig. 8 and which demonstrates the presence of a high-quality $c(26\times2)$ HOC phase. An angular distribution recorded after measuring the energy-loss spectrum (not shown) was practically identical. In Fig. 8 we compare a He-atom energy-loss spectrum recorded at an angle of incidence of 36° (curve *A*) to the corresponding spectrum reported by Zeppenfeld *et al.*[7] (curve *B*). The positions and intensities of the peaks at ±2.5 and ±5.1 meV, single and double annihilations, and excitations of the transverse *S* mode are in good agreement with the previous results.[7] However, the important mode at 3.75 meV seen by Zeppenfeld *et al.*[7] is missing in our data. We have recorded He-atom energy-loss spectra also at a number of different angles of incidence and also for Xe adlayers with different (lower density) structures, but in no case were we able to observe the feature at around 3.75 meV. In order to resolve this surprising inconsistency we have investigated the influence of coadsorbed CO on the structural and dynamical properties of the $c(26\times2)$ phase. To this end we have exposed a clean, perfect Xe $c(26\times2)$ adlayer to CO at a surface temperature of $T_S=50$ K by backfilling the chamber to a pressure of 5×10^{-8} mbar for different amounts of time. As can be seen in the inset (B) of Fig. 9, the influence of the coadsorbed CO molecules on the lateral structure is rather weak, and the angular distribution recorded after exposures of 1.2 L ($1\ \mathrm{L}=1\times10^{-6}$ mbar s) is virtually identical to that for the perfect $c(26\times2)$ overlayer. In Fig. 9 a TOF spectrum of the clean Xe surface is compared with spectra recorded

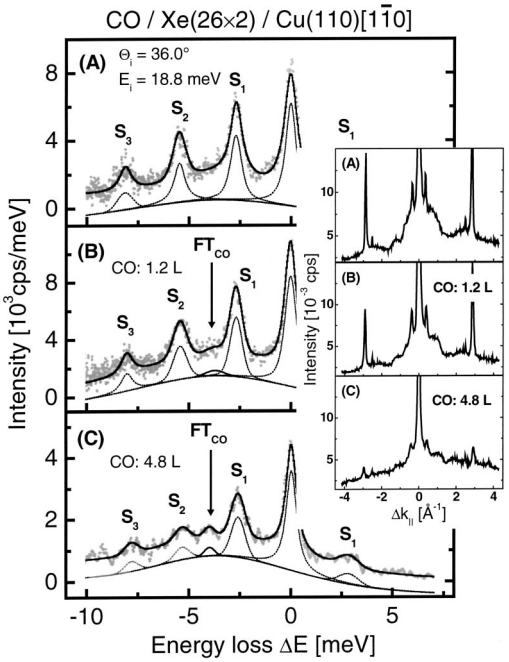

FIG. 9. Series of TOF spectra recorded at a He-atom incident energy of $E_i = 18.8$ meV and an incident angle of $\Theta_i = 36.0°$ (similar to the spectrum shown in Ref. 23) for a contamination-free Xe surface (A) and after coadsorption of 1.2 L (B) and 4.8 L (C) CO at a sample temperature of 50 K. The arrow marks the loss peak related to the excitation of the frustrated CO vibration parallel to the surface. Inset: influence of the CO adsorption on the Xe HOC diffraction scans.

after CO exposures of 1.2 and 4.8 L. As can be seen in the spectra (B) and (C), the adsorption of CO leads to the formation of a new energy-loss peak located at $\Delta E = 3.7$ meV (labeled FT_{CO}). This energy is identical to that seen after CO adsorption on the clean Cu(110) surface[24] and, in accordance with previous work,[24] we assign this mode to the CO frustrated translation parallel to the Cu(110) surface.

IV. DISCUSSION

The structural properties reported here for the most stable of the Xe overlayers on Cu(110) in the monolayer and submonolayer regime, the $c(26\times2)$ phase, are in excellent agreement with the previously reported results by Zeppenfeld *et al.*[14] and Ramseyer *et al.*[23] In contrast to the previous work, however, the present results for the dynamical properties demonstrate that the Xe $c(26\times2)$ overlayer on Cu(110) exhibits a dispersive adsorbate vibrational mode at energies below the S_1 mode which shows significant dispersion. The situation is thus similar to the case of the other two low-indexed Cu surfaces, the $(\sqrt{3}\times\sqrt{3})R30°$ Xe monolayer on Cu(111) and the hexagonal incommensurate Xe adlayer on Cu(100) (Refs. 2 and 3). Similar to the other two surfaces, this longitudinal vibration exhibits a rather small excitation probability in inelastic He-atom scattering. As has been discussed in connection with a detailed theoretical analysis, this fact can be related to the longitudinal character of this mode, which leads to a much weaker coupling than in the case of the transversely (normal to the surface) polarized S_1 mode.[19,22]

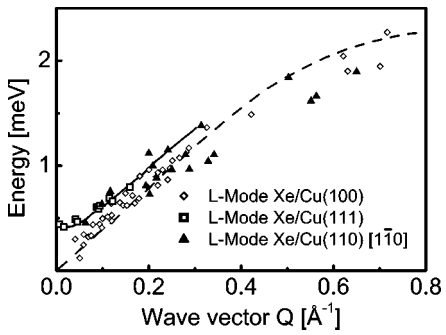

FIG. 10. Comparison of the experimental *L*-mode dispersion (solid triangles) for the Cu(110) surface with the corresponding results for other low-index Cu surfaces, Cu(111) with a commensurate Xe overlayer (squares), and Cu(100) with an incommensurate Xe adlayer adsorbed (rhombs). The solid and dashed line are dispersion curves fitted to the phonon peak positions related to the Xe/Cu(111) and Xe/Cu(100) systems (Refs. 3 and 35).

Before proceeding with the discussion of the *L* mode, we briefly note that the present findings are inconsistent with the previous report on the dynamical properties of this surface by Zeppenfeld *et al.*[7] and Ramseyer *et al.*[23] In these works a peak was seen in the experimental He-atom TOF spectra which carried about the same intensity as the S_2 mode. Such a large excitation probability is inconsistent with the longitudinal character of this mode.[19,22] In an attempt to reproduce the earlier data we recorded TOF spectra under the same kinematical conditions as were used in the previous experiments. These results, which have been published in a previous Comment[25] and which are compiled in Fig. 8, demonstrate that we are able to reproduce all features of the spectrum (including the S_1 and S_2 modes) except the mode at 3.75 meV. Under the conditions of this spectrum the intensity of the *L* mode should be at least about one order of magnitude weaker than that of the S_1 mode: e.g., with the signal-to-noise ratio in spectrum *B* in Fig. 8 the *L* mode would be hardly visible. Since we observe an intense mode at 3.7 meV after coadsorption of CO, we assign the previously observed mode at 3.75 meV to a CO-induced vibration (see above and Ref. 25).

As for the Xe monolayers on Cu(111) and Cu(100), the *L* mode is significantly softer than expected from the Xe-Xe gas-phase potential. Although a full lattice dynamical analysis has not been carried out for the present case, a comparison of the *L* mode (see Fig. 10) dispersion for the Cu(110) surface with that seen for Cu(111) and Cu(100) indicates that also in the present case the force constant that couples the adjacent Xe atoms is reduced to about 30% of the precise HFD-B2 gas-phase potential, which yields force-constant-coupling nearest-neighbor Xe atoms of $\beta_R^{\mathrm{HFD}} = (\partial^2/\partial^2 r)V(r) = 1.67\ \mathrm{N\,m^{-1}}$ (Ref. 26).

One possible origin of the significant decrease of the radial Xe-Xe force constant is an exchange-induced sidewise displacement of the surface electron charge upon Xe physisorption, as discussed in Ref. 27. An investigation of the *L*-mode dispersion curves for the Cu(110) surface is of spe-

cial interest since this surface exhibits a twofold symmetry only. Along the $[1\bar{1}0]$ direction, the Xe adlayer structure is high-order commensurate, and as a result, the *L*-mode energy at the $\bar{\Gamma}$ point (so-called zone-center phonon gap) is very small. In the [001] direction, on the other hand, the unit cell is much smaller and a phonon gap is expected for the *L* mode, in analogy to the results presented previously for the $(\sqrt{3}\times\sqrt{3})R30°$ Xe overlayer on Cu(111). Indeed, the experimental data reveal a gap at the $\bar{\Gamma}$ point of 0.55 ± 0.15 meV. As has been shown previously,[28] this energy can be used to estimate the corrugation of the Xe-Cu potential energy surface $V(r)$. Reduced to the [001] direction only,

$$V(y)=E_B(e^{-2\alpha(z-z_0)}-2e^{-\alpha(z-z_0)}) + U_{0y}[1-\cos(k_y y)]e^{-\alpha(z-z_0)}, \quad (1)$$

where E_B denotes the total Xe-Cu binding energy, U_{0y} the activation barrier for diffusion, and k_y the reciprocal lattice vector. The parameter α can be calculated from the *S*-mode energy $\omega_S=E_S/\hbar$ and the particle mass *M* according to

$$\alpha=[M\omega_S^2/(2E_B)]^{-1/2}, \quad (2)$$

and U_{0y} can be estimated from the zone-center gap energy $\omega_L(0)=E_L(0)/\hbar$ via

$$U_{0y}=M\omega_L(0)^2/k_y^2. \quad (3)$$

Using the experimental value of $\omega_L(0)=0.55\pm0.15$ meV, we obtain a total corrugation of $U_{0y}=3.1\pm0.8$ meV. Note that this experimental value is considerably smaller (about 80%) than the theoretical result given by Dienwiebel *et al.*, which was obtained by a summation over pairwise Lennard-Jones potentials.[29]

The observation of the *L* mode along both high-symmetry directions is also relevant for an independent assignment of the modes. The assignment of the *L* mode to the longitudinal mode in the Xe overlayer for Cu(111) and Cu(100) has recently been challenged by Bruch,[4] who noted that the experimental energies coincide with that of the shear-horizontal mode (SH mode) of the Xe adlayer. Whereas for Cu(100) the situation is complicated by the fact that the Xe domains are rotated relative to the substrate by 30% (Ref. 30), for the $(\sqrt{3}\times\sqrt{3})R30°$ structure of Xe on Cu(111) a coupling of the He atoms to the SH mode can be excluded on the basis of symmetry selection rules. In the present case of the $c(26\times2)$ overlayer of Xe on Cu(110), the longitudinal and shear-horizontal modes can be uniquely distinguished by their energy at the $\bar{\Gamma}$ point. Along the $[1\bar{1}0]$ direction the longitudinal mode should exhibit no or only a very small zone-center gap, whereas the SH mode is expected to show a finite value. Along the [001] direction the situation is reversed. In fact, at the $\bar{\Gamma}$ point the SH mode along $[1\bar{1}0]$ and the longitudinal mode along [001] are identical, as well as the SH mode along [001] and the longitudinal mode along $[1\bar{1}0]$. The fact that we observe a small but finite zone-center phonon gap for the *L* mode along the [001] direction thus unambiguously supports our assignment of the weak, dispersive mode to the longitudinal mode in the Xe adlayer.

V. SUMMARY

Spectra recorded for the Xe monolayer at low incident He energies allow us to extract information on the longitudinal Xe phonon dispersion curve. In the present high-resolution He-atom energy-loss study we have clearly observed a highly dispersive vibrational mode with energies below the first excitation energy of the transverse Einstein-like Xe monolayer vibration in both high-symmetry directions of the Cu(110) substrate. Along the [001] direction the experimental data reveal an energy gap at the $\bar{\Gamma}$ point of 0.55 ± 0.15 meV, which allows us to unambiguously assign this mode to the longitudinal *L* mode.[31,32] The *L* mode of the Xe monolayer on Cu(110) is significantly softer than expected from the Xe-Xe gas-phase potential. The good agreement with the *L*-mode dispersion seen for Xe monolayers on Cu(111) and Cu(100) (Refs. 2 and 3) indicates that in the present case, in contrast to the previous results reported for the Xe/Cu(110) system, the force constant between adjacent monolayer Xe atoms is reduced to about 30% of the gas-phase potential, which yields a force constant of $\beta_R^{\mathrm{HFD}}=(\partial^2/\partial^2 r)V(r)=1.67\ \mathrm{N\,m^{-1}}$ (Ref. 26). On the basis of the present results we can rule out that the mode at 3.75 meV observed by Ramseyer *et al.*[23] and Zeppenfeld *et al.*[6,7] is an intrinsic feature of the Xe monolayer. A likely explanation is the presence of a coadsorbed species, as we could show by coadsorption of CO on the high-ordered commensurate $c(26\times2)$ Xe surface.

[1] L. W. Bruch, M. W. Cole, and Z. Zaremba, *Physical Adsorption: Forces and Phenomena* (Oxford University Press, New York, 1997).

[2] J. Braun, D. Fuhrmann, A. Siber, B. Gumhalter, and C. Wöll, Phys. Rev. Lett. **80**, 125 (1998).

[3] A. P. Graham, M. F. Bertino, F. Hofmann, J. P. Toennies, and C. Wöll, J. Chem. Phys. **106**, 6194 (1997).

[4] L. W. Bruch, J. Chem. Phys. **107**, 4443 (1997).

[5] L. W. Bruch, A. P. Graham, and J. P. Toennies, J. Chem. Phys. **112**, 3314 (2000).

[6] P. Zeppenfeld, K. Kern, R. David, K. Kuhnke, and G. Comsa, Phys. Rev. B **38**, 12329 (1988).

[7] P. Zeppenfeld, M. Buchel, R. David, G. Comsa, C. Ramseyer, and C. Girardet, Phys. Rev. B **50**, 14667 (1994).

[8] B. J. Hinch, A. Lock, H. H. Madden, J. P. Toennies, and G. Witte, Phys. Rev. B **42**, 1547 (1990).

[9] D. M. Smilgies and J. P. Toennies, Rev. Sci. Instrum. **59**, 2185 (1988).

[10] B. J. Hinch, D. R. Frankl, and W. Allison, Surf. Sci. **180**, 2 (1987).

[11] U. Harten, J. P. Toennies, and C. Wöll, J. Chem. Phys. **85**, 2249 (1986).
[12] R. M. Slayton, C. M. Aubuchon, T. L. Camis, A. R. Noble, and N. J. Tro, J. Phys. Chem. **99**, 2151 (1995).
[13] C. Xu, B. E. Koel, and M. T. Paffett, Langmuir **10**, 166 (1994).
[14] P. Zeppenfeld, M. Buchel, J. Goerge, R. David, G. Comsa, C. Ramseyer, and C. Girardet, Surf. Sci. **366**, 1 (1996).
[15] T. Seyller, M. Caragiu, R. D. Diehl, P. Kaukasoina, and M. Lindroos, Chem. Phys. Lett. **291**, 5 (1998).
[16] T. Seyller, M. Caragiu, and R. D. Diehl, Surf. Sci. **454**, 55 (2000).
[17] B. F. Mason and B. R. Williams, Surf. Sci. **130**, 295 (1983).
[18] A. Siber, B. Gumhalter, P. G. Graham, J. P. Toennies, Phys. Rev. B **63**, 115411 (2001).
[19] B. Gumhalter, Phys. Rep. **351**, 1 (2001).
[20] A. Siber and B. Gumhalter, Surf. Sci. **502–503**, 422 (2002).
[21] F. Hofmann, J. P. Toennies, and J. R. Manson, J. Chem. Phys. **101**, 10155 (1994).
[22] A. Siber, B. Gumhalter, J. Braun, A. P. Graham, M. F. Bertino, J. P. Toennies, D. Fuhrmann, and C. Wöll, Phys. Rev. B **59**, 5898 (1999).
[23] C. Ramseyer, V. Pouthier, C. Girardet, P. Zeppenfeld, M. Buchel, V. Diercks, and G. Comsa, Phys. Rev. B **55**, 13203 (1997).
[24] J. Braun, J. Weckesser, J. Ahner, D. Mocuta, J. T. Yates, and C. Wöll, J. Chem. Phys. **108**, 5161 (1998).
[25] C. Boas, T. Becker, M. Kunat, U. Burghaus, and C. Wöll, Phys. Rev. B **64**, 037401 (2001).
[26] A. K. Dham, W. J. Meath, A. R. Allnatt, R. A. Aziz, and M. J. Slaman, Chem. Phys. **142**, 173 (1990).
[27] P. S. Bagus, V. Staemmler, and C. Wöll, Phys. Rev. Lett. **89**, 096104 (2002).
[28] B. N. J. Persson and A. Nitzan, Surf. Sci. **367**, 261 (1996).
[29] M. Dienwiebel, P. Zeppenfeld, J. Einfeld, G. Comsa, F. Picaud, C. Ramseyer, and C. Girardet, Surf. Sci. **446**, 1 (2000).
[30] M. A. Chesters and J. Pritchard, Surf. Sci. **28**, 460 (1971).
[31] R. E. Allen, G. P. Alldredge, and F. W. d. Wette, Phys. Rev. B **4**, 1648 (1971).
[32] R. E. Allen, G. P. Alldredge, and F. W. d. Wette, Phys. Rev. B **4**, 1661 (1971).
[33] A. Glachant and U. Bardi, Surf. Sci. **87**, 187 (1979).
[34] C. Ramseyer, C. Girardet, P. Zeppenfeld, J. Goerge, M. Buchel, and G. Comsa, Surf. Sci. **313**, 251 (1994).
[35] L. W. Bruch, Phys. Rev. B **37**, 6658 (1988).